MUC21 induces the viability and migration of glioblastoma via the STAT3/AKT pathway

LEIBO WANG[1], XUEBIN ZHANG[2], JUN LIU[1] and QINGJUN LIU[1]

Departments of [1]Neurosurgery and [2]Pathology, Tianjin Huanhu Hospital, Tianjin 300350, P.R. China

Received June 5, 2021; Accepted January 17, 2022

DOI: 10.3892/etm.2022.11260

Abstract. Glioblastoma (GBM) is a malignant tumor with one of the fastest increasing morbidity and mortality rates. As such, more therapeutic targets need to be developed to combat this disease. Mucin 21 (MUC21) is a human counterpart of mouse epiglycanin and mediates multiple cellular functions. However, its possible effects on GBM and its possible mechanism remain unclear. The current study aimed to clarify the role or MUC21 in the progression of GBM by performing a series of *in vitro* assays, including Cell Counting Kit-8, colony formation, wound closure, transwell, and *in vivo* assays. In the present study, the aberrantly high expression of MUC21 in human GBM tissues and cell lines was observed and it was revealed that it was associated with the clinicopathological feature, tumor recurrence, in patients with GBM. MUC21 promoted the viability and motility of GBM cells *in vitro* and stimulated tumor growth *in vivo*. It was further confirmed that MUC21 promoted the progression of GBM via the STAT3/AKT pathway and it was considered that MUC21 could serve as a promising target for the treatment of GBM.

Introduction

Glioblastoma (GBM) is a malignant tumor with one of the most rapidly increasing morbidity and mortality rates, making it become a great threat to human life and health (1). To improve the life quality of patients, the pathologic type and clinical stage of GBM should be clearly defined (2). It was also revealed that GBM is prone to early metastasis (3). Several novel therapeutic methods for tumors have been established, such as immunotherapy and targeted therapy (4). In recent years, positive progress has been made towards targeted therapy for GBM, where multiple targeted therapeutic drugs have been developed clinically or are currently in clinical trials (5). However, to combat this disease, more potential therapeutic targets are required.

Mucin 21 (MUC21) is known to be the human counterpart of mouse epiglycanin (6), which has 98 tandem repeats of 15 amino acids and three exceptional repeats, followed by the stem domain, transmembrane domain and the cytoplasmic tail (7). It was reported that MUC21 mediates multiple cellular functions such as cell adhesion (8). Notably, the membranous expression of MUC21 has been identified in cancer cells (9).

Importantly, the role of MUC21 in the progression and metastasis of cancer has already been revealed (9). MUC21 has been found to be widely expressed in multiple types of tissues and highly expressed in the micropapillary elements of lung adenocarcinomas (9). In addition, MUC21 modulates the adhesion of tumor cells (7). A recent study indicated that MUC21 was a critical regulator in the incohesive growth pattern in lung adenocarcinoma (9). However, the possible effects of MUC21 on GBM cells and the regulatory mechanisms underlying them remain unclear.

The present study aimed to investigate the expression of MUC21 in GBM tissues and cell lines, and to explore its role in GBM progression, further revealing its mechanism.

Materials and methods

Patients. Human GBM tissues and corresponding adjacent non-cancerous tissues (5 mm from the tumor site; 47 paired) in the present study were obtained from Chinese patients (Han nationality) with GBM at the Tianjin Huanhu Hospital (Tianjin, China) who received only surgical resection with no other chemical or radiation therapies from February 2018 to January 2021. The present study was approved by the Ethics Committee of Tianjin Huanhu Hospital (Tianjin, China). All patients provided written informed consent. The clinicopathological features, such as patient age, sex, tumor tumor location (supratentorial or sub-tentorial), recurrence and isocitrate dehydrogenase [NADP(+)] mutation are listed in Table I. Written formal consent was obtained from all recruited patients for the use of these samples for research purposes.

Immunohistochemistry (IHC). To explore the expression levels of MUC21 in tumor tissues and corresponding adjacent non-cancerous tissues of patients with GBM, IHC assays were

Correspondence to: Dr Leibo Wang, Department of Neurosurgery, Tianjin Huanhu Hospital, 6 Jizhao Road, Tianjin 300350, P.R. China
E-mail: wangliliqiang@sina.cn

Key words: glioblastoma, mucin 21, prognosis, vaibility, STAT3/AKT pathway

performed. Tumor tissues were resected, embedded in paraffin and then cut into 5-μm slices. The sections were deparaffinized with xylene and rehydrated using a descending ethanol series. Sections were then fixed with 4% paraformaldehyde (PFA) at 25˚C for 30 min and subsequently incubated with 2% BSA (Beyotime Institute of Biotechnology) for 30 min at room temperature. Slides were then incubated with MUC21 antibody (1:100; cat. no. NBP3-06591; Novus Biologicals, LLC) for 2 h at room temperature. Following primary incubation, sections were incubated with biotinylated secondary antibody (1:200; cat. no. NB7158; Novus Biologicals, LLC) at room temperature for another 1 h. Samples were subsequently stained with diaminobenzidine and observed under a light microscope (Carl Zeiss AG).

The scoring method was briefly described as follows. The proportion of cells with positive staining was graded: 0, negative stained tumor cells; 1, <25% positive stained cells; 2, 25-50% positive stained cells and 3, >50% positive stained cells. The staining intensity was assessed on a score of 0 (no staining), 1 (moderate) and 2 (strong). The expression level of MUC21 was calculated as follows: Positive staining tumor cells score x staining intensity score. A staining index of 0-2 was considered as low expression, whereas 3, 4 and 6 were considered as high expression.

Cell culture and transfection. Human GBM cell lines, U251 (cat. no. MZ-0186), U87 (glioblastoma of unknown origin; cat. no. MZ-2007; both from Ningbo Mingzhou Biotechnology Co., Ltd.) and U373 (cat. no. CRL-2741™; American Type Culture Collection) were obtained from the indicated companies and STR profiling was performed for these cell lines. The cell lines were maintained in Dulbecco's modified Eagle medium (DMEM; Invitrogen; Thermo Fisher Scientific, Inc.) supplemented with 10% fetal bovine serum (FBS; Gibco; Thermo Fisher Scientific, Inc.) and maintained in a 5% CO_2 incubator at 37˚C.

MUC21 short hairpin RNA (shRNA; sequence: 5'-GGG TCAGCATAGTCACCAACT-3' and 5'-GCGCTCTGACAT GCAGAA-3') and negative control shRNA (shNC; sequence: 5'-TTCTCCGAACGTGTCACGT-3') plasmids were purchased from Santa Cruz Biotechnology, Inc. and transfected into both U251 and U87 cells using Lipofectamine® 3000 (Invitrogen; Thermo Fisher Scientific, Inc.). shNC was used as a control to compare with MUC21 shRNA (1 μg) transfection. pcDNA3.1-MUC21 was used for overexpression assays and the pcDNA3.1-vector (Addgene, Inc.) was used as control. A total of $1x10^5$ cells were seeded into six-well plates and 0.5 μg plasmids were used for transfection. The cells were transfected using 10 μl Lipofectamine® 3000 (Invitrogen; Thermo Fisher Scientific, Inc.) in each well. Cells were cultured for 4 h with Lipofectamine®/plasmid mix at 37˚C and the transfection was completed. Subsequent assays were performed after 24 h.

Reverse transcription-quantitative PCR assay. To extract total RNA from U87 and U251 cells, TRIzol® (cat. no. 15596026; Invitrogen; Thermo Fisher Scientific, Inc.) reagent was used. Total RNA was reverse transcribed into cDNA at 42˚C for 1 h using M-MLV reverse transcriptase (cat. no. M1701; Promega Corporation, includes M-MLV 5X Reaction Buffer 5 μl, dNTP, 10 mM 1.25 μl, Recombinant RNasin® Ribonuclease Inhibitor 25 units, M-MLV RT 200 units and Nuclease-Free Water to final volume of 25 μl).

qPCR was then performed using the SYBR Ex Taq kit (cat. no. 638319; Takara Bio, Inc.) and used according to the manufacturer's protocol. MUC21 expression levels were normalized to the relative level of GAPDH. The following primer pairs were used: MUC21 forward, 5'-CTTCCCATAGTGCATCTA CTGC-3' and reverse, 5'-GAACCAGTTAGGACTCCACCT GGGCC-3'; and GAPDH forward, 5'-GGTCGTATTGGG CGCCTGGT-3' and reverse, 5'-TACTCAGCGCCAGCATCG CC-3'. The relative mRNA level of MUC21 was derived from triplicate reactions. The following thermocycling conditions were used: Initial denaturation at 95˚C for 3 min; followed by 30 cycles of denaturation at 95˚C for 30 sec, annealing at 58˚C for 30 sec and extension at 72˚C for 30 sec. The $2^{-\Delta\Delta Cq}$ method was used to quantify the results (10).

Western blotting. Proteins were extracted from U87 cells using RIPA lysis buffer (Cell Signaling Technology, Inc.). The BCA assay method was used for protein concentration determination, after which proteins were separated (20 μg per lane) by 8% SDS-PAGE. The proteins were transferred onto a PVDF membrane, which was subsequently blocked in 5% BSA at room temperature for 2 h in TBST with 0.5% Tween and incubated with specific antibodies against MUC21 (1:1,000), β-actin (1:10,000; cat. no. ab8227; Abcam), anti-Ki67 (1:1,000; cat. no. ab15580; Abcam), anti-proliferating cell nuclear antigen (PCNA; 1:1,000; cat. no. 2586; Cell Signaling Technology, Inc.), anti-MMP2 (1:1,000; cat. no. 40994; Cell Signaling Technology, Inc.), anti-MMP9 (1:1,000; cat. no. 13667; Cell Signaling Technology, Inc.) STAT3 (1:1,000; cat. no. ab68153; Abcam), p-STAT3 (1:1,000; cat. no. ab267373; Abcam), AKT (1:1,000; cat. no. ab8805; Abcam) and phosphorylated (p)-AKT (1:1,000; cat. no. Ab38449; Abcam) at 25˚C for 2 h. The membranes were then incubated at room temperature with HRP-conjugated anti-mouse IgG (cat. no. 7076) and anti-rabbit IgG (cat. no. 7074; both from Cell Signaling Technology, Inc.) secondary antibodies (1:3,000) for 1 h at room temperature. Signals were visualized using an ECL kit (Beyotime Institute of Biotechnology). ImageJ (version 1.8.0; National Institutes of Health) was used for densitometry.

Colony formation assay. U87 and U251 cells (1,000/well) transfected with control or MUC21 shRNA plasmids were plated into six-well culture plates. Cells were maintained using DMEM with 10% FBS. Colonies were considered to consist of >100 cells. After 2 weeks, cell colonies were fixed with PFA at room temperature for 25 min and stained with 0.1% crystal violet at 25˚C for 20 min. After washing with PBS twice, the number of colonies was manually counted.

MTT assay. U87 and U251 cells at a density of ~1,000 cells per well were plated into 96-well plates and maintained for 24 h. MTT (0.5 mg/ml) was added into the plate for 4 h at 25˚C and then removed to extract the stained cells. Dimethyl sulfoxide (200 μl) was used to dissolve the purple formazan. The OD value in each well was measured using a microplate reader at a wavelength of 570 nm.

Wound closure assay. U87 and U251 cells were cultured for 24 h, after which a wound was made using 20-μl pipette tips.

Table I. Relationship between MUC21 expression and clinicopathological characteristics of patients with glioblastoma (n=47).

Clinicopathological characteristic	Total (n=47)	Expression level of MUC21		Chi-square value	P-value
		Low	High		
Sex				0.002	0.966
Female	14	5	9		
Male	33	12	21		
Age, years				0.093	0.760
<60	18	7	11		
≥60	29	10	19		
Tumor lateralization				1.877	0.171
Supratentorial	14	3	11		
Subtentorial	33	14	19		
Recurrence				4.821	0.028
No	21	4	17		
Yes	26	13	13		
Isocitrate dehydrogenase [NADP(+)] mutations				5.895	0.863
No	36	13	23		
Yes	11	4	7		

MUC21, mucin 21.

Samples were then washed with PBS to remove debris and serum-free DMEM was added to stimulate healing. Images were captured at 0 and 24 h timepoints using a light microscope and the extent of wound closure was calculated.

Tumor growth assays. All animal procedures were approved by the Institutional Animal Care and Use Committee of Tianjin Huanhu Hospital (approval no. 2019-0002). A total of 8 female nude mice (8 weeks old and weighing 18-20 g, 4 mice per group were used) were purchased from the Experimental Center of Beijing Vital River Laboratory Animal Technology Co., Ltd. The mice were housed in an air conditioning-regulated environment (20˚C and 40% humidity). Mice were kept under a 12 h light/dark cycle with *ad libitum* access to food and water. The mice were anesthetized in acrylic chambers. Anesthesia was induced by inhalation of 2.5% isoflurane and 1% isoflurane was used for maintenance. Then the mice were placed in the right lateral decubitus position. Briefly, ~5x10^5 U251 cells stably transfected with control or MUC21 shRNA plasmids in 50 μl of PBS with 50 μg of growth factor-reduced Matrigel were injected into the left lateral thorax of the mice at the lateral dorsal axillary line. Additionally, the tumor grew subcutaneously in the abdomen of the nude mice, at the injection site. After 14 days, the tumor volume was monitored every 7 days. After 49 days, mice were weighed, anesthetized with sodium pentobarbital (60 mg/kg, intraperitoneally) and then sacrificed by cervical dislocation. Subsequently, all tumors were isolated, measured, their images were captured and the tumor growth curves were exhibited and analyzed. Tumor volume was calculated using the following formula: Volume=(length x width x height)/2.

Statistical analysis. GraphPad 5.0 software (GraphPad Software, Inc.) was used for statistical analysis in the present study. Results were presented as the mean ± SD (n=3). The associations between clinicopathological features of patients with GBM and MUC21 expression were analyzed using χ^2 analysis. Statistical differences between two groups were analyzed by paired student's t-test. ANOVA followed by Dunnett's post hoc test was used for multiple comparisons. P<0.05 was considered to indicate a statistically significant difference.

Results

MUC21 levels are upregulated in GBM tissues and are associated with clinical features. To analyze the role of MUC21 in the progression of GBM, MUC21 expression levels in tumor tissues and adjacent tissues from patients with GBM were detected (Fig. 1A). The results revealed that GBM tissue had higher MUC21 expression levels compared with normal adjacent tissue. Subsequently, the levels of MUC21 in three types of GBM cells (U251, U87 and U373) were investigated. It was revealed that MUC21 protein levels were markedly enhanced in U251 and U87 cells, compared with U373 cells (Fig. 1B). In addition, the IHC assay revealed high MUC21 expression levels in GBM tissues, with arrows indicating high and low expression areas (Fig. 1C). Compared with patients with low expression of MUC21, no significant association between the sex, age, tumor lateralization and isocitrate dehydrogenase mutations of patients and the expression level of MUC21 was observed. By contrast, MUC21 expression was significantly associated with recurrence (P=0.028; Table I). Therefore, the enhanced MUC21

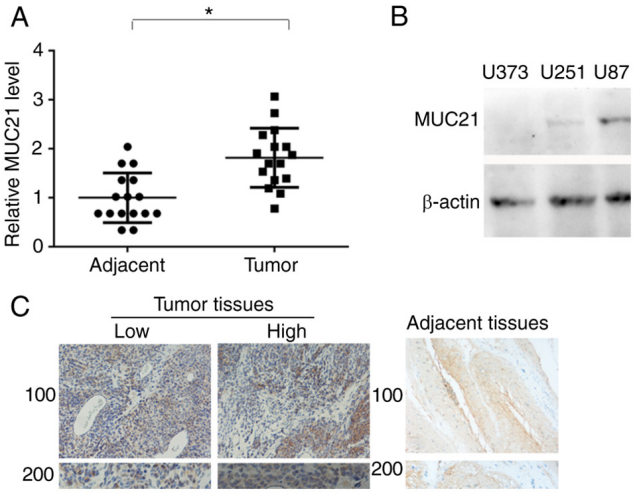

Figure 1. MUC21 is highly expressed in human GBM tissues. (A) A reverse transcription-quantitative PCR assay were conducted to determine the mRNA levels of MUC21 in GBM and corresponding adjacent non-cancerous tissues. A paired Student's t-test was used for the analysis of tumor and adjacent non-tumor samples. (B) Western blotting was performed to determine MUC21 expression in three GBM cell lines. (C) Immunohistochemistry was performed to evaluate the protein levels of MUC21 in GBM tumor and corresponding adjacent non-cancerous tissues. Magnification, x100 and x200 (scale bar, 5 mm). *P<0.05 as indicated. GBM glioblastoma; MUC21, mucin 21.

expression in GBM tissues and its association with clinical features of patients with GBM was deduced.

MUC21 expression is downregulated in U251 and U87 cells with MUC21 shRNA transfection. To determine the potential role of MUC21 in GBM progression, MUC21 expression was decreased by shRNA plasmids to reveal its biological function in GBM cell lines. After transfecting MUC21 or control shRNA into U251 and U87 cells, RT-qPCR analysis revealed that MUC21 expression levels were reduced (Fig. 2A). Similarly, western blot analysis demonstrated a reduction of MUC21 protein levels following the transfection of MUC21 shRNA plasmids (Fig. 2B). Therefore, transfection of MUC21 shRNA effectively downregulated MUC21 mRNA and protein levels.

MUC21 promotes GBM cell viability and migration in vitro. To assess the effects of MUC21 in GBM progression, the viability of U251 and U87 cells was evaluated by colony formation and MTT assays after silencing MUC21. The results revealed that cell viability was significantly reduced after the depletion of MUC21, with the decreased colony number and OD value at 570 nm (Fig. 3A and B). Subsequently, wound closure assays revealed the effects of MUC21 on the migration of GBM cells. It was observed that MUC21 silencing significantly reduced wound closure in U251 and U87 cells (Fig. 3C). Furthermore, western blotting revealed that the expression levels of two proliferation cell markers, Ki67 and PCNA, were decreased in both U251 and U87 cells after MUC21 shRNA transfection (Fig. 3D). Decreased expression levels of MMP2 and MMP9, which are necessary for tumor cell migration, were also revealed after MUC21 depletion (Fig. 3E). Collectively, it was demonstrated that MUC21 expression contributes to cell proliferation and migration of GBM *in vitro*.

MUC21 contributes to the progression of GBM via the STAT3 and AKT signaling pathway. To investigate the signaling proteins that are involved in MUC21-mediated GBM progression, the impact of MUC21 depletion on the STAT3 and AKT pathway in GBM cells was examined. U251 cells were transfected with MUC21 shRNA or MUC21 overexpressing plasmid for 72 h, after which phosphorylated STAT3 and AKT were assessed by western blot analysis. MUC21 shRNA transfection resulted in the decrease of phosphorylated STAT3 and AKT. In addition, the total protein levels of STAT3 and AKT were not altered upon MUC21 depletion in GBM cells (Fig. 4A). Conversely, MUC21-overexpressing U251 cells exhibited accumulated levels of phosphorylated tyrosine proteins STAT3 and T308 phosphorylated AKT (Fig. 4B). These results suggested that MUC21 modulated STAT3 and AKT activation in GBM cells.

MUC21 stimulates GBM progression through the STAT3 and AKT pathways in vivo. To evaluate the importance of MUC21 in GBM progression *in vivo*, a xenograft assay was performed to explore the role of MUC21 in the tumor growth of mice. Control or MUC21-depleted U251 cells were injected into nude mice to induce tumor growth. The tumor volume was monitored every week from the 2nd to 7th week. Finally, tumors were isolated and images were captured. No difference in murine weight was observed between the two groups (Fig. 5A). As exhibited in Fig. 5A, tumor images were displayed. A relatively slow tumor growth rate was observed in MUC21-depleted group compared with the control group (Fig. 5A). There was no significant difference of the murine body weight between the two groups after the experiment (data not shown). The knockdown efficiency of MUC21 in isolated tumors was further confirmed through an IHC assay (Fig. 5B).

Similarly, decreased expression levels of MUC21, MMP2, PCNA, p-AKT and p-STAT3 were identified following MUC21 knockdown in tumor tissues (Fig 5C). In conclusion, it was revealed that MUC21 stimulates GBM progression through the STAT3 and AKT pathway *in vivo*.

Discussion

Recently, a series of advances have been made in the targeted therapy of GBM. There are specific therapeutic targets that are available for the different pathological types of GBM, which have been established clinical use or are currently in clinical trials (11). For this type of malignant tumor, which carries a high morbidity and mortality, targeted therapy is undoubtedly the most effective treatment to supplement or even replace traditional treatment, such as surgical resection, chemo- and radiotherapy (12). To improve the survival of patients with GBM at advanced stages, the development of new targeted therapeutic drugs are urgently required. In the present study, it was revealed that an MUC family protein, MUC21, was highly expressed in patients with GBM and was associated with the tumor recurrence of patients. The present study suggested the involvement of MUC21 in GBM progression and it was

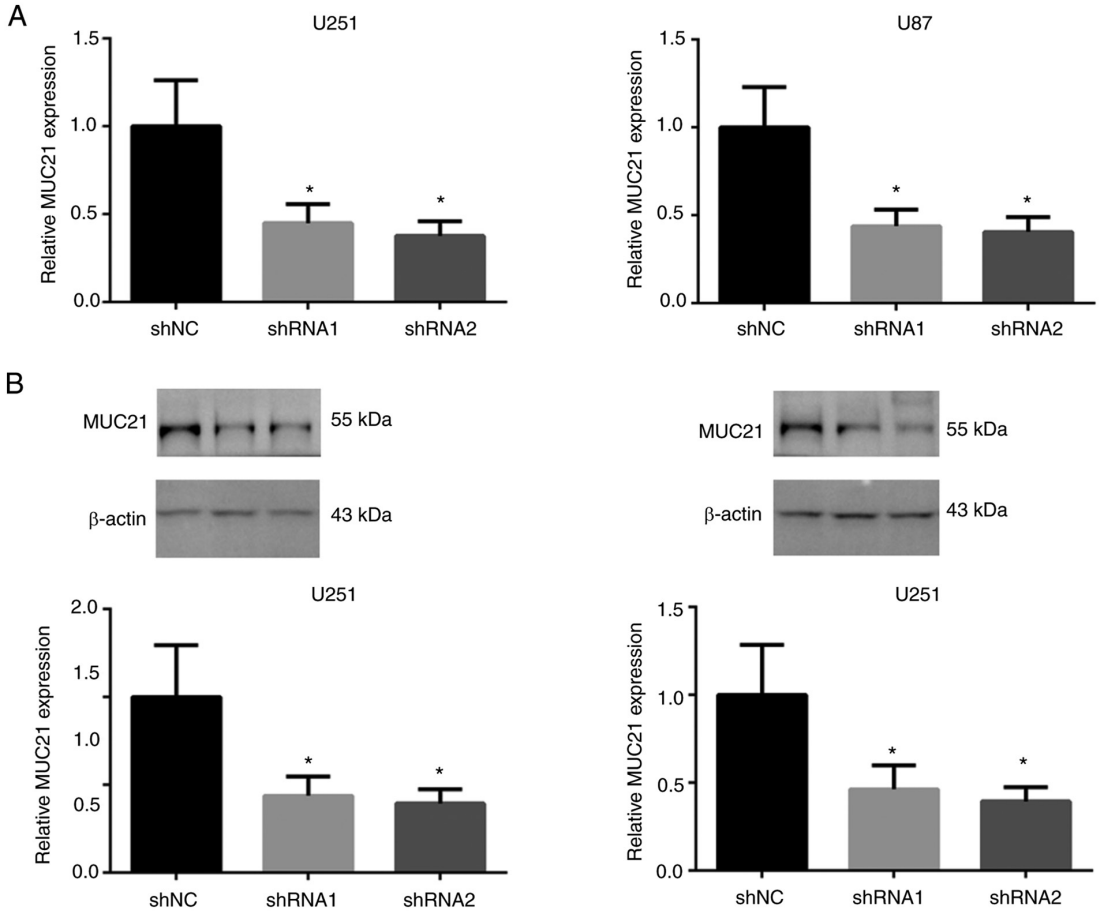

Figure 2. MUC21 expression is downregulated in U251 and U87 cells after MUC21 shRNA transfection. (A) Reverse transcription-quantitative PCR assays were performed to measure MUC21 mRNA levels in U251 and U87 cells following control or MUC21 shRNA transfection. (B) Western blot analysis was performed to determine the protein expression of MUC21 in U251 and U87 cells following control or MUC21 shRNA transfection. *P<0.05 vs. shRNA. MUC21, mucin 21; NC, negative control; shRNA, short hairpin RNA.

considered that MUC21 could serve as a potential therapeutic target for the disease.

MUC21, previously named epiglycanin, was identified as a glycoprotein located on the surface of TA3-Ha cells. It was also determined to be a critical member of Mucin family, which contains several tumor regulators such as MUC15 (13). Mucins have been revealed to play key roles in lung cancer progression and affect the diagnostic, prognostic and therapeutic implications of multiple types of tumors (6,9,14). MUC21, having a specific glycosylation status, may be involved in the progression of EGFR-mutated lung cancer, particularly at the stage where tumors are transforming from pure lepidic to micropapillary tumors through low papillary lepidic lesions (9). Specific expression of MUC21 in micropapillary elements of lung adenocarcinomas has been revealed, which suggests an associaton between MUC21 expression and the progression of EGFR-mutated lung adenocarcinomas (15). MUC21 inhibitors have potential to serve as drugs in the treatment of multiple types of cancers, such as lung cancer and esophageal carcinomas (15). However, the precise mechanism requires further study. Additionally, MUC21 expression was also found in the cytoplasm of GBM cells via developing a specific antibody targeting the cytoplasmic tail of MUC21 (16). Through this antibody, the aforementioned study revealed the high expression of MUC21 in GBM tissues compared with adjacent normal tissues. Similarly, the aberrantly high expression of MUC21 in human GBM tissues was also observed in the present study, and it was identified that MUC21 expression was positively associated with the clinicopathological features of patients with GBM, in consistency with the previous data (15). Therefore, these data, together with the present findings, revealed that MUC21 has clinical potential as a serum biomarker and therapeutic target for patients with GBM.

Overexpression experiments have been previously performed to verify the effects of MUC21 on GBM cells. Notably, it was found that MUC21 promoted GBM cell proliferation and migration (Wang *et al*, unpublished data). In the present study, focus was addressed on the influence of MUC21 depletion on GBM cells, suggesting that it may be used as a potential therapeutic target for GBM.

Through MTT and colony formation assays, the effects of MUC21 on GBM cell viability were identified. The present data further confirmed that MUC21 promoted the migration of GBM cells. These results revealed the oncogenic role of MUC21 in GBM progression *in vitro*. In addition, through the present *in vivo* study, it was demonstrated that the depletion of MUC21 inhibited the tumor growth of GBM cells in mice, further confirming *in vitro* data. Furthermore, it was determined that MUC21 promoted the progression of GBM by regulating the AKT pathway.

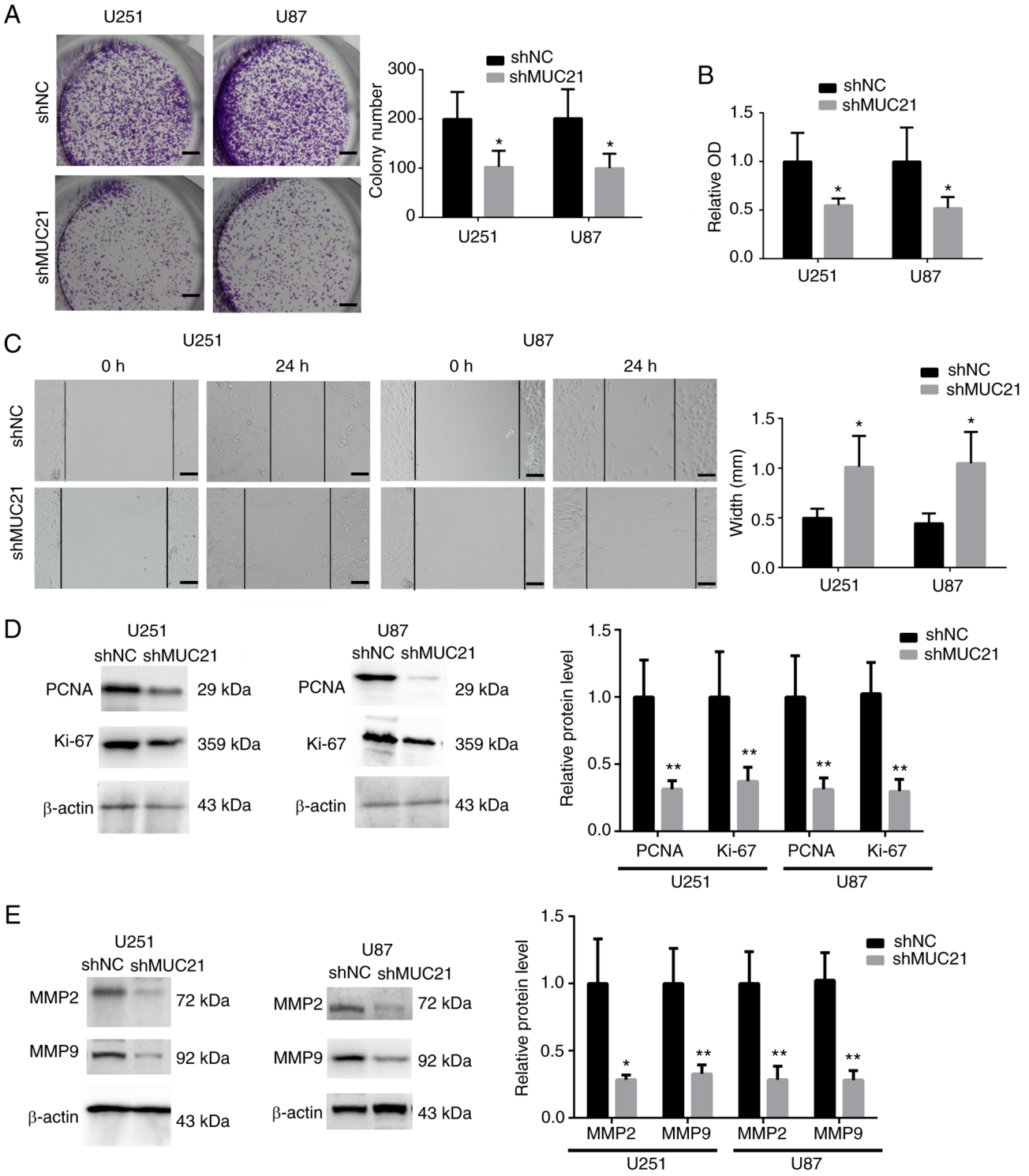

Figure 3. MUC21 promotes GBM cell viability and migration *in vitro*. (A) Cell viability was assessed after MUC21 depletion in U87 and U251 through colony formation assays. (B) MTT assays were performed to detect the viability of cells transfected with the indicated shRNA. (C) Wound closure assay of GBM cells transfected with the indicated shRNA were performed for the quantification of migrated cells after 24 h. Magnification, x200. Western blotting assays were performed to analyze the expression of (D) Ki-67 and PCNA, and (E) MMP2 and MMP9 in GBM cells transfected with the indicated shRNA. Relative expression was analyzed. *P<0.05 and **P<0.01 vs. the shNC group. GBM glioblastoma; MUC21, mucin 21; PCNA, proliferating cell nuclear antigen; shRNA, short hairpin RNA; NC, negative control.

The decreased degree of cell adhesion may affect tumor metastasis by promoting cell invasion and spreading through the regulation of lymphatics (16). Notably, Yi *et al* (7) revealed that MUC21 inhibited cell-extracellular matrix interactions and interfered with intercellular adhesions, which suggested that MUC21 suppressed intercellular adhesion molecules and surface integrins (6). Additionally, MUC21 also affected the immune response (9,17,18). In the present study, the effects of MUC21 on the migration and invasion of GBM cells, possibly through the effect on cell adhesion, were also identified.

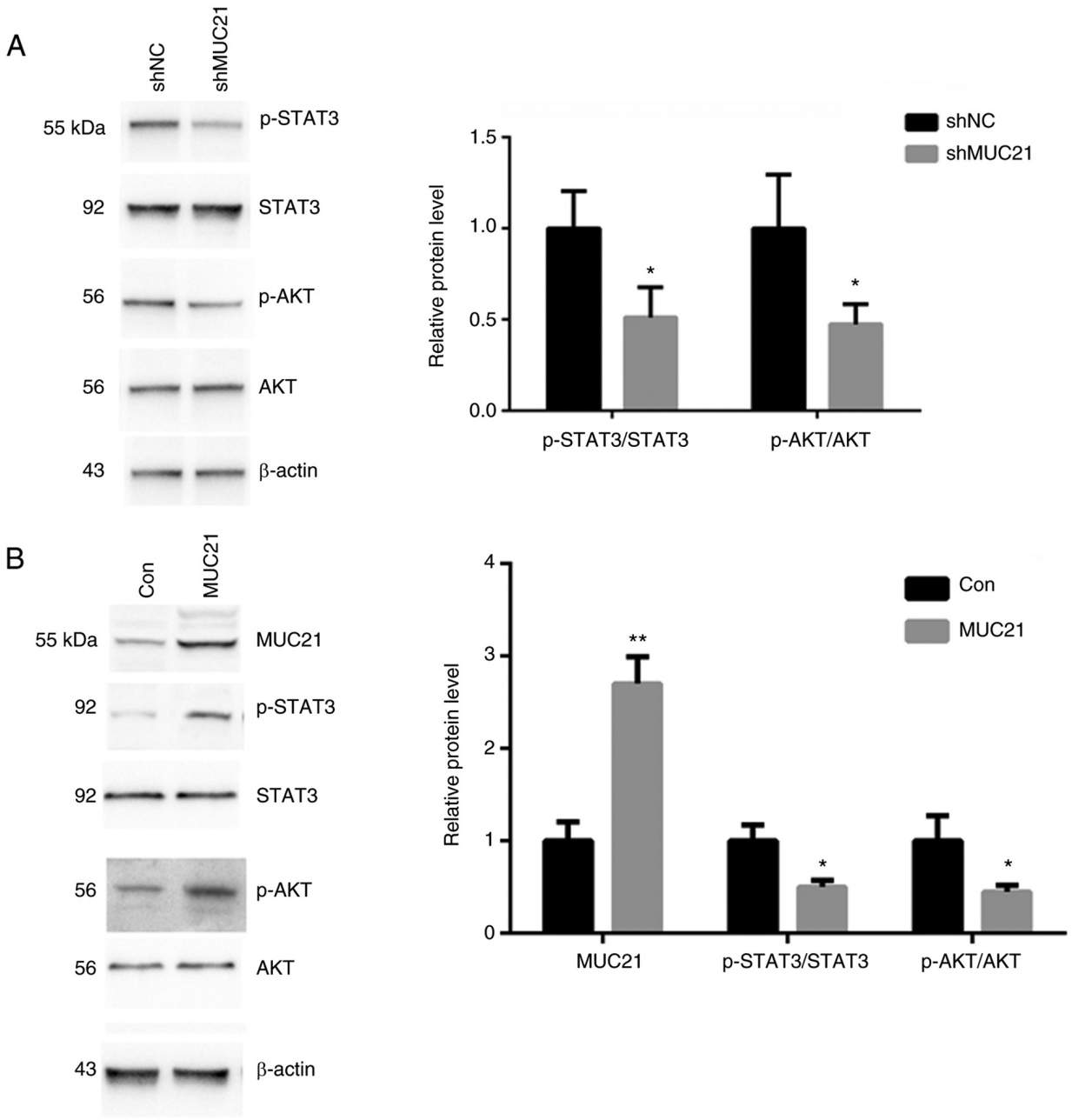

Figure 4. MUC21 contributes to GBM progression via the STAT3 and AKT signaling pathway. (A) The protein levels of p-STAT3, STAT3, p-AKT and AKT in shMUC21-transfected or control U251 cells were detected by immunoblot assays. (B) The protein levels of MUC21, p-STAT3, STAT3, p-AKT and AKT in MUC21-overexpressing or control U251 cells were detected by immunoblot assays. The relative expression was analyzed. *P<0.05 and **P<0.01 vs. shNC or Con. Con, control; MUC21, mucin 21; NC, negative control; p-, phosphorylated; shRNA, short hairpin RNA.

The STAT3/AKT axis is widely involved in the regulation of various physiological and pathological processes (19,20). It has multiple effects on a variety of tumors, including lung cancer (21). In addition, the STAT3/AKT axis has been determined to mediate the migration, invasion and metastasis of tumors (10,20,21-23). Notably, the present data revealed that MUC21 promoted the migration and invasion of GBM cells via the STAT3/AKT axis, which provided new evidence of MUC21 as an effective therapeutic target for GBM.

Nevertheless, the lack of examination of the expression of p-STAT3 and p-AKT on patient tissues is a potential limitation of the present study. In fact, the tumor samples that were kept were paraffin specimens. Due to the lack of fresh samples, western blot assays were not performed.

Several studies have previously revealed that MUC21 was abnormally expressed in human GBM tissues and was associated with poor patient prognosis (9,17,18). However, to the best of our knowledge, no studies have provided evidence that MUC21 inhibitors were developed. In future studies, inhibitors of MUC21 should be developed and their possible effects on GBM progression should be investigated.

In the present study, the high expression of MUC21 in human GBM tissues and cells was revealed. The expression of MUC21 was associated with the tumor recurrence of patients

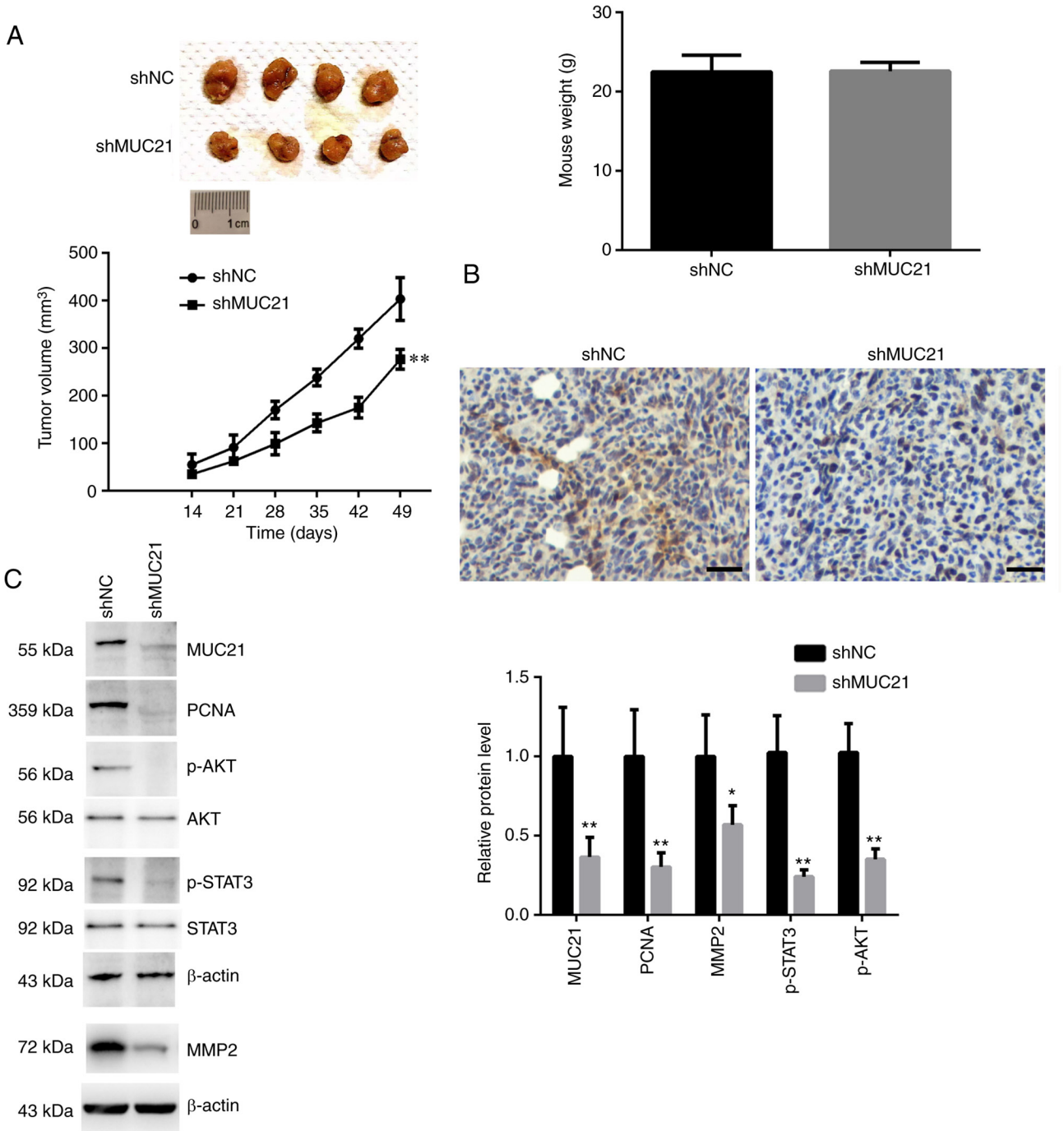

Figure 5. MUC21 stimulates glioblastoma progression through the STAT3 and AKT pathway *in vivo*. (A) U251 cells stably transfected with control or MUC21 shRNA vectors were subcutaneously implanted into nude mice. Tumor volume was monitored every week. Isolated tumors were displayed in (A). Tumor growth curves were compared between control and MUC21 depletion groups. Murine weight was also measured. (B) An immunohistochemistry assay was conducted to assess MUC21 protein levels in control or MUC21-depleted groups (scale bar, 200 μm). (C) Western blotting assays were performed to assess the expression levels of the indicated proteins in control or MUC21-depleted tumor tissues isolated from nude mice. *P<0.05 and **P<0.01 vs. shNC. MUC21, mucin 21; NC, negative control; PCNA, proliferating cell nuclear antigen; p-, phosphorylated; shRNA, short hairpin RNA.

with GBM. It was further found that MUC21 contributed to the viability, migration and invasion of GBM cells via the STAT3/AKT axis and that it promoted tumor growth in mice. Collectively, it was considered that MUC21 could serve as a promising therapeutic target for GBM treatment.

Acknowledgements

Not applicable.

Funding

No funding was received.

Availability of data and materials

The datasets used and/or analyzed during the current study are available from the corresponding author on reasonable request.

Authors' contributions

LW, XZ, JL and QL carried out molecular biology experiments and drafted the manuscript. LW, XZ, JL and QL designed the study and performed statistical analysis. LW, XZ, JL and QL conceived the study, participated in its design, coordinated the study and drafted the manuscript. JL and QL confirm the authenticity of all the raw data. All authors have read and approved the final version of the manuscript.

Ethics approval and consent to participate

All animal procedures and patient-derived tissue experiments performed in the current study were approved by the Ethics Committee of Tianjin Huanhu Hospital (Tianjin, China). Written informed consent was provided by all patients.

Patient consent for publication

Not applicable.

Competing interests

The authors declare that they have no competing interests.

References

1. Park JE, Kim HS, Lee J, Cheong EN, Shin I, Ahn SS and Shim WH: Deep-learned time-signal intensity pattern analysis using an autoencoder captures magnetic resonance perfusion heterogeneity for brain tumor differentiation. Sci Rep 10: 21485, 2020.
2. Dai S, Yan Y, Xu Z, Zeng S, Qian L, Huo L, Li X, Sun L and Gong Z: SCD1 confers temozolomide resistance to human glioma cells via the Akt/GSK3β/β-catenin signaling axis. Front Pharmacol 8: 960, 2018.
3. Kig C, Beullens M, Beke L, Van Eynde A, Linders JT, Brehmer D and Bollen M: Maternal embryonic leucine zipper kinase (MELK) reduces replication stress in glioblastoma cells. J Biol Chem 288: 24200-24212, 2013.
4. Mahasenan KV and Li C: Novel inhibitor discovery through virtual screening against multiple protein conformations generated via ligand-directed modeling: A maternal embryonic leucine zipper kinase example. J Chem Inf Model 52: 1345-1355, 2012.
5. Zhao Y, Zhao Z, Cui Y, Chen X, Chen C, Xie C, Qin B and Yang Y: Redox-responsive glycosylated combretastatin A-4 derivative as novel tubulin polymerization inhibitor for glioma and drug delivery. Drug Develop Res 82: 1063-1072, 2021.
6. Yoshimoto T, Matsubara D, Soda M, Ueno T, Amano Y, Kihara A, Sakatani T, Nakano T, Shibano T, Endo S, *et al*: Mucin 21 is a key molecule involved in the incohesive growth pattern in lung adenocarcinoma. Cancer Sci 110: 3006-3011, 2019.
7. Yi Y, Kamata-Sakurai M, Denda-Nagai K, Itoh T, Okada K, Ishii-Schrade K, Iguchi A, Sugiura D and Irimura T: Mucin 21/epiglycanin modulates cell adhesion. J Biol Chem 285: 21233-21240, 2010.
8. Tian Y, Denda-Nagai K, Kamata-Sakurai M, Nakamori S, Tsukui T, Itoh Y, Okada K, Yi Y and Irimura T: Mucin 21 in esophageal squamous epithelia and carcinomas: Analysis with glycoform-specific monoclonal antibodies. Glycobiology 22: 1218-1226, 2012.
9. Kai Y, Amatya VJ, Kushitani K, Kambara T, Suzuki R, Tsutani Y, Miyata Y, Okada M and Takeshima Y: Mucin 21 is a novel, negative immunohistochemical marker for epithelioid mesothelioma for its differentiation from lung adenocarcinoma. Histopathology 74: 545-554, 2019.
10. Livak KJ and Schmittgen TD: Analysis of relative gene expression data using real-time quantitative PCR and the 2(-Delta Delta C(T)) method. Methods 25: 402-408, 2001.
11. Guo P, Yu Y, Li H, Zhang D, Gong A, Li S, Liu W, Cheng L, Qiu Y, Yao W, *et al*: TGF-â1-induced miR-503 controls cell growth and apoptosis by targeting PDCD4 in glioblastoma cells. Sci Rep 7: 11569, 2017.
12. Ganguly R, Hong CS, Smith LG, Kornblum HI and Nakano I: Maternal embryonic leucine zipper kinase: Key kinase for stem cell phenotype in glioma and other cancers. Mol Cancer Ther 13: 1393-1398, 2014.
13. Chen T, Chen Z, Lian X, Wu W, Chu L, Zhang S and Wang L: MUC 15 Promotes osteosarcoma cell proliferation, migration and invasion through livin, MMP-2/MMP-9 and Wnt/β-catenin signal pathway. J Cancer 12: 467-473, 2021.
14. Ratan C, Cicily K D D, Nair B and Nath LR: MUC Glycoproteins: Potential biomarkers and molecular targets for cancer therapy. Curr Cancer Drug Targets 21: 132-152, 2021.
15. Matsumura M, Okudela K, Nakashima Y, Mitsui H, Denda-Nagai K, Suzuki T, Arai H, Umeda S, Tateishi Y, Koike C, *et al*: Specific expression of MUC21 in micropapillary elements of lung adenocarcinomas-implications for the progression of EGFR-mutated lung adenocarcinomas. PLoS One 14: e0215237, 2019.
16. Cao H, Ye D, Zhao Q, Luo J, Zhang S and Kong J: A novel aptasensor based on MUC-1 conjugated CNSs for ultrasensitive detection of tumor cells. Analyst 139: 4917-4923, 2014.
17. Zhang L, Strouthos CG, Wang Z and Deisboeck TS: Simulating brain tumor heterogeneity with a multiscale agent-based model: Linking molecular signatures, phenotypes and expansion rate. Math Comput Model 49: 307-319, 2009.
18. Itoh Y, Kamata-Sakurai M, Denda-Nagai K, Nagai S, Tsuiji M, Ishii-Schrade K, Okada K, Goto A, Fukayama M and Irimura T: Identification and expression of human epiglycanin/MUC21: A novel transmembrane mucin. Glycobiology 18: 74-83, 2008.
19. Zhang Z, Sun C, Li C, Jiao X, Griffin BB, Dongol S, Wu H, Zhang C, Cao W, Dong R, *et al*: Upregulated MELK leads to doxorubicin chemoresistance and M2 macrophage polarization via the miR-34a/JAK2/STAT3 pathway in uterine leiomyosarcoma. Front Oncol 10: 453, 2020.
20. Zhang M, Liu Q, Mi S, Liang X, Zhang Z, Su X, Liu J, Chen Y, Wang M, Zhang Y, *et al*: Both miR-17-5p and miR-20a alleviate suppressive potential of myeloid-derived suppressor cells by modulating STAT3 expression. J Immunol 186: 4716-4724, 2011.
21. Lv X, Wang L and Zhu T: MiR-20a-5p suppressed TGF-β1-triggered apoptosis of human bronchial epithelial BEAS-2B cells by targeting STAT3. Mol Cell Probes 50: 101499, 2020.
22. Shang J, Li Y, Yin G, Li Z, Jiang L and Bai Q: Phosphatidylinositol 3,4,5-trisphosphate-dependent rac exchanger 2 protein facilitates glioma progression via Akt and Stat3 signaling. J Mol Neurosci 71: 1674-1682, 2021.
23. Kim HI, Lee SJ, Choi YJ, Kim MJ, Kim TY and Ko SG: Quercetin induces apoptosis in glioblastoma cells by suppressing Axl/IL-6/STAT3 signaling pathway. Am J Chin Med 49: 767-784, 2021.